Quantum Chemistry Study of Li^+−1,2-Dimethoxypropane Complexes

Grant D. Smith* and Kerri Crain

Department of Chemical Engineering, University of Missouri-Columbia, Columbia, Missouri 65211

Richard L. Jaffe

NASA Ames Research Center, Moffett Field, California 94035

Received: August 30, 1996; In Final Form: December 18, 1996[⊗]

Quantum chemistry studies of the lowest energy conformers of 1,2-dimethoxypropane (DMP) complexes with Li^+ ions have been carried out. Results of these calculations are compared with those of our recent study of Li^+−1,2-dimethoxyethane (DME) complexes. Because of a chiral center, conformation space is more complex for DMP than for the structurally similar but achiral DME. Qualitatively similar behavior to that seen previously in studies of DME is found, however, including the presence of low-energy conformers containing consecutive gauche dihedrals of opposite sense and stronger interactions of the Li^+ ion with conformers containing O-C−C-O gauche conformations. The former is a result of stabilization of conformers by attractive 1,5 $CH_3\cdots O$ electrostatic interactions, while the latter reflects the ability of the ion to interact with both ether oxygen atoms. The calculated Li^+−DMP complex energies and geometries reveal that favorable interactions of the α methyl group with the ion result in a $Li^+-t\bar{g}t$ complex energy comparable that of the Li^+-tgt complex. Comparison of calculated Raman spectra with experimental measurements on DMP/$LiClO_4$ solutions indicates an increasingly high population of the $t\bar{g}t$ conformer with increasing salt content.

Introduction

The conformational properties of poly(alkyl ethers) and the influence of solvents and ions on the polymer conformations are of great interest. In previous work, we demonstrated that careful ab initio electronic structure calculations performed on dimethoxymethane and 1,3-dimethoxydimethyl ether,[1] 1,2-dimethoxyethane (DME),[2] and 1,3-dimethoxypropane[3] provide important insight into the conformational characteristics of these model molecules for the respective polymers poly(oxymethylene),[4] poly(oxyethylene)[5,6] (POE), and poly(oxytrimethylene).[3] In the quantum chemistry study of DME,[2] we found the *ttt* , *tgt*, and tg^+g^- conformers all to be of low energy. These conformers are illustrated in Figure 1. We concluded that the high gauche fraction of the O-C−C-O dihedral in DME as determined from gas phase NMR vicinal coupling experiments is due, to a large extent, to the low energy of the tg^+g^- conformers and is not the result of a *tgt* conformer being 0.5−1.0 kcal/mol lower in energy than the *ttt* conformer, as has been widely held.[2] On the basis of the DME conformer energies and geometries obtained from quantum chemistry, we developed a third-order rotational isomeric state (RIS) model that accurately predicts the conformations of unperturbed POE chains.[6] The quantum chemistry data were also used in parametrizing an atomistic force field for DME and POE[5] that has been utilized in molecular dynamics simulations of DME liquid[7] and POE melts.[8,9] Most recently, we have used quantum chemistry to study the geometry and energetics of complexes of Li^+, Cl^-, and I^- ions with model ethers, including DME.[10] Currently, we are completing a quantum chemistry and molecular mechanics study of diglyme, a longer POE model molecule corresponding to three ether repeat units.[11]

In a recent paper concerning the conformational properties of poly(propylene oxide) (PPO), results of quantum chemistry calculations on the model molecule 1,2-dimethoxypropane (DMP) were reported.[12] The study concentrated on the important question of the effects of solvent on the conformer populations of DMP in an effort to explain large differences in NMR vicinal coupling constants for DMP as measured in the gas phase and in various solvents.[12,13] DMP conformational geometries were determined using a modest basis set at the SCF level. Solvation effects were approximated using the self-consistent reaction field (SCRF) approach. Conformer free energies were determined for the gas phase and various solvents (SCRF method) using correlated methods and larger basis sets, and conformer populations were estimated.

In this work we continue our investigation of the conformational properties of poly(alkyl ethers) by reporting on the results of a detailed quantum chemistry study of complexes of the most

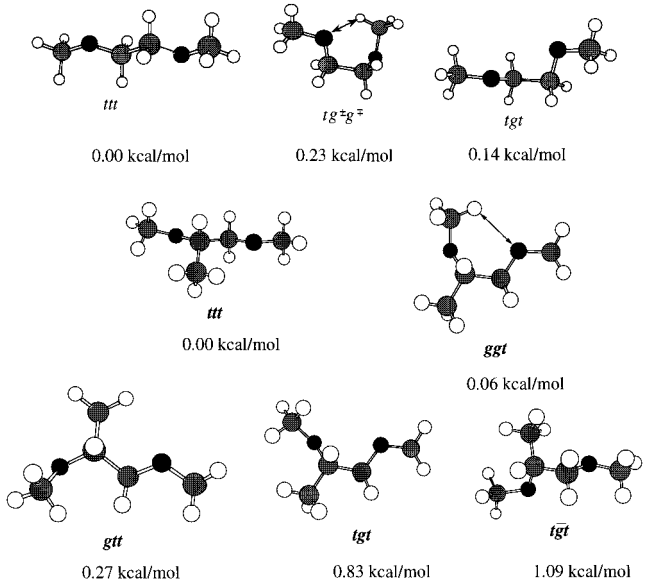

Figure 1. Low-energy conformers of 1,2-dimethoxyethane and 1,2-dimethoxypropane. Energies are MP2/D95+(2df,p) values relative to the respective *ttt* conformers. Values for DME are from ref 2. Important 1,5 $CH_3\cdots O$ interactions are indicated.

[⊗] Abstract published in *Advance ACS Abstracts,* March 15, 1997.

S1089-5639(96)02670-9 CCC: $14.00

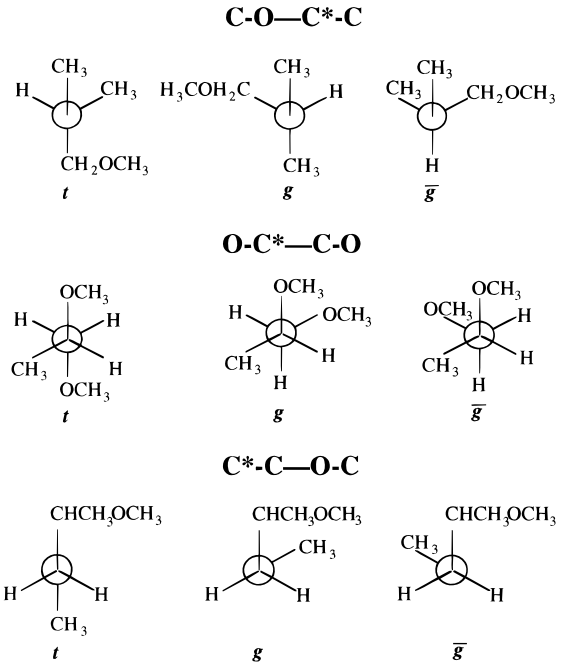

Figure 2. Conformations of the C-O−C*-C, O-C*−C-O, and C*-C−O-C dihedrals in 1,2-dimethoxypropane. The interaction associated with each conformation is also shown.

important conformers of DMP with Li^+. It is known from Raman spectroscopy that the presence of lithium salts strongly perturbs the conformations of DMP and PPO,[14] and investigation of this effect is a goal of this work. Our calculations, carried out at a high level of theory consistent with our previous study of DME[2] and Li^+−DME complexes, allow us to directly compare DMP conformer and complex energies with those of DME. We have determined the geometries of the most important DMP conformers and their complexes with Li^+ at both the SCF and MP2 levels. We have generated Raman spectra based upon quantum chemistry normal-mode analysis for the DMP conformers and Li^+−DMP complexes and have compared these results with experiment.

1,2-Dimethoxypropane

Quantum Chemistry Calculations. In our previous work, the optimized geometries and conformer energies of all 10 unique conformers of DME conformer were determined.[2] In DMP, the methyl (α) substituent results in a chiral center (C*) and nonequivalent gauche conformations of the backbone torsions, yielding 27 unique conformers. Following standard notation, the C-O−C*-C and O-C*−C-O gauche conformations are labeled *g* and $\bar{g}$. The respective arrangements are illustrated in Figure 2. For the C*-C−O-C dihedral, we label the gauche conformation which, when O-C*−C-O is trans, brings the end methyl group into a pentane-type interaction with the methyl substituent, *g*, and the opposite rotation $\bar{g}$. We determined optimized geometries for 14 DMP conformers at the SCF level using a D95** basis set and for six conformers at the MP2 level using the same basis set. Full geometry optimizations were performed for each DMP conformer and Li^+−DMP complex, and each molecule or complex had C_1 symmetry because of the chiral center. Simple RIS arguments indicate that the remaining 13 DMP conformers are of higher energy due to unfavorable steric effects and account for an inconsequentially small fraction of the total conformer population.[12] The optimized backbone dihedral angles ϕ_1 = C-O−C*-C, ϕ_2 = O-C*−C-O, and ϕ_3 = C*-C−O-C and the dihedral angle ϕ_4 = C-C*−O-C, which involves the methyl side group, are compared for the SCF and MP2 geometries in Table 1 (t = 180°). Note that the sense of the torsional angle ϕ_4 is uniquely defined by the backbone conformation and the stereochemical configuration of the molecule. Conformer energies, relative to the energy of the *ttt* conformer, were determined using the D95** basis set and the larger D95+(2df,p) basis set both at the SCF level and with the Møller−Plesset second-order perturbation correction (MP2) for electron correlation effects for most cases. The reader is referred to our earlier work[2] for details on quantum chemistry calculations and the basis sets employed. The relative conformer energies are given in Table 2. All calculations were performed using the quantum chemistry codes MULLIKEN[15] and GAUSSIAN94.[16] The calculations were performed on IBM RS6000 workstations at the NASA Ames Research Center and at the University of Missouri-Columbia and a Cray C90 at the San Diego Super Computer Center.

TABLE 1: Geometries of Low-Energy Conformers of 1,2-Dimethoxypropane

conformer	ϕ_1[a]	ϕ_2	ϕ_3	ϕ_4
ttt	−157.3	175.5	179.9	−62.1
	−165.3	*176.1*	*180.1*	*−61.5*
ggt	−92.5	69.8	−177.2	170.7
	−76.5	*76.5*	*−178.9*	*−165.2*
gtt	−91.0	173.2	178.6	−66.9
	−86.5	*173.1*	*178.2*	*−67.9*
tgt	−144.6	72.1	−174.3	−166.4
	−149.7	*74.3*	*−173.2*	*−164.4*
tḡt	−164.4	−72.6	175.9	52.1
	−168.9	*−74.8*	*176.4*	*49.4*
tḡg	−162.7	−74.8	84.7	49.9
	−166.7	*−79.1*	*75.8*	*45.3*
gḡt	−75.4	−65.9	179.3	55.4
tgḡ	−153.0	68.5	−98.2	−169.3
ttḡ	−164.4	176.5	−85.8	−61.0

[a] Torsional angles are defined in the text. Numbers in italics are from MP2 geometries.

TABLE 2: Energies of Low-Energy Conformers of 1,2-Dimethoxypropane

	energy (kcal/mol)					
	D95** SCF Geometry				D95** MP2 Geometry	
	D95**		D95+(2df,p)		D95**	D95+(2df,p)
conformer	SCF	MP2	SCF	MP2	MP2	MP2
ttt	0.00	0.00	0.00	0.00	0.00	0.00
ggt	0.46	−0.03	0.55	0.04	−0.15	0.06
gtt	0.31	0.26	0.29	0.24	0.23	0.27
tgt	1.06	1.00	0.86	0.76	1.04	0.83
tḡt	1.98	1.44	1.76	1.10	1.41	1.09
tḡg	2.13	0.66	2.43	0.96	0.43	0.87
gḡt	2.00		1.79	1.01		
tgḡ	1.69		1.85	1.15		
ttḡ	1.75		1.89	1.32		
ḡtt	2.71		2.95	2.42		
gḡg	2.51		2.82	1.21		
gtḡ	2.26		2.34	1.78		
ggg	2.44		2.65	1.45		
ḡḡt	3.48[a]					

[a] This conformer is a saddle point.

DMP Conformer Energies. As was found for DME,[2] both basis set completeness and electron correlation effects strongly influence the relative conformer energies in DMP, as can be seen by examining Table 2. The largest differences between conformer energies determined using the D95+(2df,p) and the smaller D95** basis set are for the *tgt* and *tḡt* conformers: the relative energies of these conformers decrease by about 0.25−0.35 kcal/mol at the MP2 level when the larger basis set is employed. The corresponding basis set effect was around 0.5

kcal/mol for the DME *tgt* conformer.[2] We demonstrated previously that it is the inclusion of the additional polarization functions in the D95+(2df,p) basis set that has the greatest effect on the DME *tgt* energy.[2] Our conformer energies cannot be compared with the results of the previous DMP study, where 6-31G* and 6−311+G* basis sets were employed,[12] because only relative conformer *free* energies are reported therein. We have demonstrated for DME[2] and other model ethers[1,3] that improvements in the basis set beyond D95+(2df,p) and treatments of electron correlation beyond MP2 do not significantly influence the relative conformer energies. We have estimated MP2/D95+(2df,p) conformer energies to be accurate to within about ±0.3 kcal/mol for the model alkyl ether molecules.[2] This conclusion is supported by recent IR studies of DME in the gas phase.[17] In this work, the energy of the tg^+g^- DME conformer was determined to be 0.3 kcal/mol relative to the *ttt* conformer, quite close to our quantum chemistry value of 0.2 kcal/mol.

The four lowest energy conformers of DMP, plus the $t\bar{g}t$ conformer, are illustrated in Figure 1. As in DME, the lowest energy conformer of DMP is the *ttt* conformer. The DMP *ggt* conformer is of nearly the same energy as the *ttt* conformer. The DMP *ggt* conformer is the analog of the DME tg^+g^- conformer in that both exhibit 1,5 $CH_3\cdots O$ interactions. These interactions are indicated in Figure 1. As in the DME tg^+g^- conformer,[2] the small steric size of the oxygen atom and attractive electrostatic interaction between a methyl hydrogen atom and the oxygen atom that is manifest in the 1,5 $CH_3\cdots O$ interactions yield a low energy for the DMP *ggt* conformer. The next lowest energy conformer in DMP is the *gtt* conformer. In DME, the energy of the gauche conformation of the C-O−C-C dihedral is relatively high compared to the trans conformation because of the unfavorable $CH_3\cdots CH_2$ gauche interaction. In DMP, the *g* conformation of C-O−C*-C dihedral also results in a $CH_3\cdots CH_2$ gauche interaction, but concurrently relieves the $CH_3\cdots CH_3$ gauche interaction between the end methyl group and the α methyl group, which occurs in the trans conformation (compare the *ttt* and *gtt* conformer in Figure 1, and also see Figure 2). The next most important DMP conformer is the *tgt* conformer. Unlike the analogous conformer in DME, the *tgt* conformer in DMP is significantly higher in energy than the *ttt* conformer. In DME, the oxygen gauche effect, which favors the gauche conformation of the O-C−C-O dihedral, is offset by unfavorable electrostatic interactions between the oxygen atoms.[2,5,6] In DMP also, the oxygen gauche effect favors a gauche arrangement of the O-C*−C-O dihedral. As in DME, this effect is offset by unfavorable electrostatic interactions between the oxygen atoms. This latter effect may be stronger in DMP than in DME.

The lowest energy conformers involving the $\bar{g}$ conformation of the O-C*−C-O dihedral are the $t\bar{g}t$, $t\bar{g}g$, and the $g\bar{g}t$ conformers. These conformers are higher in energy than the corresponding conformers with O-C*−C-O *g* conformations. The conformational restrictions associated with the O-C*−C-O $\bar{g}$ conformation and unfavorable 1,4 $CH_3\cdots O$ electrostatic interactions arising in the $\bar{g}$ conformation between the slightly negatively charged α methyl group (see below) and the backbone oxygen serve to increase the energy of the O-C*−C-O $\bar{g}$ conformation. The $t\bar{g}g$ conformer is stabilized by favorable 1,5 $CH_3\cdots O$ electrostatic interactions.

Conformer Geometries. One of the most striking features of the DMP conformer geometries is the large distortion, greater than 30° in some conformers, of the trans conformation of the C-O−C*-C dihedral, as illustrated in Table I. This is a result of large 1,4 $CH_3\cdots CH_3$ steric repulsion effects. No corresponding distortion is seen in DME. Large distortions of the gauche conformations occur in conformers in which 1,5 $CH_3\cdots O$ interactions are present. Similar distortions were seen in DME[2].

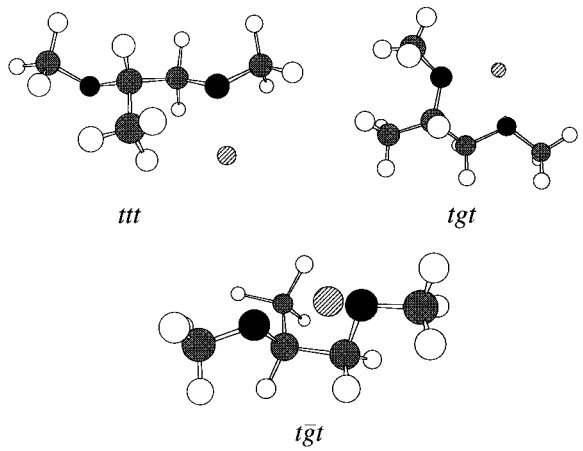

Figure 3. Optimized geometries of complexes of Li^+ and 1,2-dimethoxypropane.

TABLE 3: Geometries of Li^+−1,2-Dimethoxypropane Complexes

conformer	ϕ_1	ϕ_2	ϕ_3	Li^+−O (Å)	Li^+−O (Å)
			SCF Geometry		
Li^+−*ttt*	−149.1	−165.6	−158.3	4.207	1.804
Li^+−*tgt*	177.0	45.2	164.7	1.843	1.836
Li^+−*gtt*	−93.4	165.2	158.2	4.202	1.808
Li^+−*ggt*	−85.2	71.2	177.0	3.033	1.799
Li^+−*tḡt*	−149.7	47.8	165.5	1.838	1.848
			MP2 Geometry		
Li^+−*tgt*	176.6	46.9	165.5	1.857	1.848

We investigated the effect of optimizing geometries at the MP2 level on both the geometries and relative conformer energies for some of the most important DMP conformers. The MP2/D95** geometries are given in Table 1, and the corresponding MP2/D95**//MP2/D95+(2df,p) relative conformer energies are given in Table 2. The use of MP2 optimized geometries has only a minor effect on the relative conformer energies. The effect on the conformational geometries, however, is quite large in some cases. For example, the *t* and *g* conformations of the C-O−C*-C dihedral are noticeably closer to the "expected" values of 180° and −60° at the MP2 level.

Li^+−1,2-Dimethoxypropane Complexes

Quantum Chemistry Calculations. To investigate the influence of lithium salts on the conformations of DMP, we have calculated the geometries and energies of complexes of low-energy DMP conformers with Li^+.

Complex Geometries. Geometries of the complexes were determined at the SCF level using a D95** DMP basis set and a [8s5p3d/5s3p2d] Li basis derived previously for studies of complexes of DME and lithium salts.[10] The Li^+−DMP complex geometries are given in Table 3. We found in our study of Li^+−DME complexes that the complex geometries are a strong function of the Li basis set, but not the ether basis set, or the inclusion of electron correlation effects (see also below).[10] The Li^+−*ttt*, Li^+−*tgt*, and Li^+−*tḡt* complexes are illustrated in Figure 3. Comparing the conformer geometries in the complexes (Table 3) with those given in Table 1 for DMP alone, it can be seen that the O-C*−C-O gauche dihedral distorts significantly in the presence of Li^+. A similar effect was seen for the Li^+−*tgt* DME complex[10] and is the result of optimizing the interaction of both oxygen atoms with Li^+. The Li^+−O

TABLE 4: Energies of Li^+−1,2-Dimethoxypropane Complexes

	energy (kcal/mol)[a]					
	D95**		D95+(2df,p)			
conformer	SCF[b]	SCF[c]	SCF[b]	MP2[b]	SCF[c]	MP2[c]
Li^+−*ttt*	−42.36	−42.36				
Li^+−*tgt*	−67.20	−66.14	−64.79	−63.85(−61.87)[d]	−63.94	−63.09 (−61.11)
Li^+−*gtt*	−41.86	−41.55				
Li^+−*ggt*	−41.30	−40.84				
Li^+−*tḡt*	−68.25	−66.26	−65.81	−64.15 (−62.37)	−64.04	−63.05 (−61.27)

[a] Using SCF geometries. [b] Relative to respective conformer and Li^+ at infinite separation. [c] Relative to *ttt* and Li^+ at infinite separation. [d] Values in parentheses are BSSE corrected.

distances are given in Table 3. For the *tgt* and *tḡt* complexes, both Li^+−O distances are near the optimal Li^+−O distance of 1.835 Å for a Li^+−dimethylether complex.[10] It is also worth noting that the ϕ_1 dihedral in the Li^+−*tgt* complex is distorted by more than 30° from the value obtained for the *tgt* conformer alone. Optimizing the Li^+−*tgt* complex at the MP2 level made little difference in the geometry (see Table 3). Our previous study of Li^+−DME complexes indicated that optimization at the MP2 level made little difference in these complex geometries also.[10]

Complex Energies. The energies of the complexes, relative to the respective conformer and Li^+ at infinite separation *and* relative to the *ttt* conformer and Li^+ at infinite separation, are given in Table 4. The first values reflect the strength of the Li^+−DMP interaction, while the latter reflect the relative energies of the complexes. Energies were determined using the Li basis set described above. Our study of Li^+−DME and Li^+−dimethyl ether complexes revealed that the complex energies depend strongly on the Li basis set. For this reason we derived a new Li basis set that accurately describes the Li core electrons.[10] Also shown in Table 4 are basis set superposition error (BSSE) corrected energies for the Li^+−*tgt* and Li^+−*tḡt* complexes at the MP2 level using the larger D95+(2df,p) ether basis set. The BSSE corrections (<2 kcal/mol) are much smaller than the total binding energies. Table 4 reveals that the Li^+−*tgt* and Li^+− *tḡt* complexes are much lower in energy than the other complexes investigated. A similar effect was seen for the Li^+−*tgt* complex,[10] and reflects the favorable interaction of Li^+ with both oxygen atoms in these complexes.

The interaction of Li^+ with *tḡt* is somewhat stronger than that with *tgt*. As a result, the Li^+− *tḡt* complex may be comparable or even lower in energy than the Li^+−*tgt* complex, as reflected in Table 4, even though the *tḡt* conformer is higher in energy than the *tgt* conformer. The stronger Li^+−*tḡt* interaction may be a result of the charge distribution in DMP. Electrostatic potential calculations (D95** SCF) for DMP reveal that the end methyl groups have a net positive charge of about 0.2*e*, while the α methyl group has a slight negative charge of −0.07*e*. Consequently, the Li^+ ion has favorable electrostatic interactions with the α methyl group but interacts unfavorably with the end methyl groups. The unfavorable end methyl group−Li^+ interaction is reflected in the Li^+−*tgt* geometry. Here, the C-O−C*-C dihedral angle is about 30° larger than for *tgt*, thereby increasing the end methyl group−Li^+ distance. We also found that only the *tgt* and *tḡt* conformers would form complexes where the Li^+ ion can interact favorably with both oxygen atoms. For complexes containing gauche dihedral pairs of the opposite sense, such as *ggt*, the close proximity of the end methyl group appears to preclude such complexes and results in complexes analogous to the Li^+−*ttt* complex, where Li^+ interacts strongly with only one oxygen atom (see Tables 3 and 4). The favorable nature of the α methyl−Li^+ interaction is reflected in the Li^+−*ttt* complex geometry, as shown in Figure 3. The lowest energy Li^+−*ttt* complex geometry has the Li^+ on the same side of DMP as the α methyl, with a C−Li^+ separation of 2.38 Å. For Li^+−*tgt*, the Li^+ end methyl and α methyl distances are 2.93 and 4.04 Å, respectively, while for Li^+− *tḡt* the corresponding distances are 3.02 and 3.36 Å.

TABLE 5: Calculated Frequencies and Raman Intensities for Modes between 550 and 850 cm^{-1} for 1,2-Dimethoxypropane Complexes

	frequency	intensity	frequency (cm^{-1})		intensity
conformer	(cm^{-1}) SCF	(SCF)	SCF	MP2	(SCF)
ttt			819		8.7
Li^+−*ttt*			807		10.6
tgt			817	809	9.2
Li^+−*tgt*			780	778	8.6
gtt			829		9.8
Li^+−*gtt*			812		11.4
ggt			818		9.3
Li^+−*ggt*			819		7.6
tḡt	641	1.3	786		12.6
Li^+−*tḡt*	623	2.0	787		11.2
tḡg	642	2.5	767		12.5

Comparison with Experiment. The influence of $LiClO_4$ on the conformations of liquid DMP has been investigated via Fourier transform Raman spectroscopy.[14] The C−C and C−O bands in the 700−900 cm^{-1} range were found to be quite sensitive to salt concentration, an effect assumed to be due to changes in DMP conformations. For neat DMP, the Raman intensity in the 780−850 cm^{-1} range showed several moderately strong peaks and shoulders. This is consistent with a mixture of conformations contributing to the spectrum in this range. With increasing salt concentration, it was observed that a strong band at around 810 cm^{-1} emerges, while the peaks and shoulders observed in the spectrum of the neat liquid decrease. At the highest concentration investigated, $[Li^+]/[\text{-O-}] = 0.20$, the band at 810 cm^{-1} very much dominates the spectrum in this region. This band was associated with the *tgt* conformer (strictly speaking, the Li^+−*tgt* complex), whose population was suggested to increase with increasing salt content.

We have calculated the frequencies and Raman intensities for the most important conformers of DMP and for complexes of these conformers with Li^+. Frequencies and Raman intensities for bands in the 550−850 cm^{-1} range are given in Table 5. Frequencies and Raman intensities were calculated using a D95** ether basis set and the Li basis set described above at the SCF and MP2 (*tgt* and Li^+−*tgt* frequencies only) level using the corresponding optimized geometries. The SCF frequencies were scaled by 0.90 and the MP2 frequencies by 0.95. In the frequency range of 400−1000 cm^{-1}, differences between SCF and MP2 frequencies for *tgt* and Li^+−*tgt* are all less than 2%. Therefore, MP2 frequencies were not determined for the remaining conformers and complexes.

Examination of Table 5 reveals that all of the important DMP conformers and their complexes show strong Raman activity

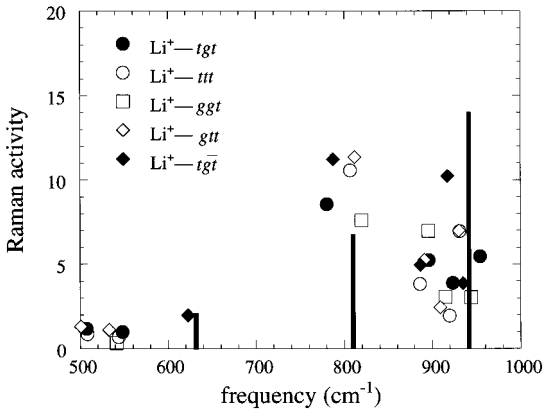

Figure 4. Raman activity for Li^+−DMP complexes in the 500−1000 cm^{-1} range. Solid lines represent relative peak heights for experimental Raman peaks in $[Li^+]/[\text{-O-}] = 0.20$ DMP/$LiClO_4$ solution (ref 14).

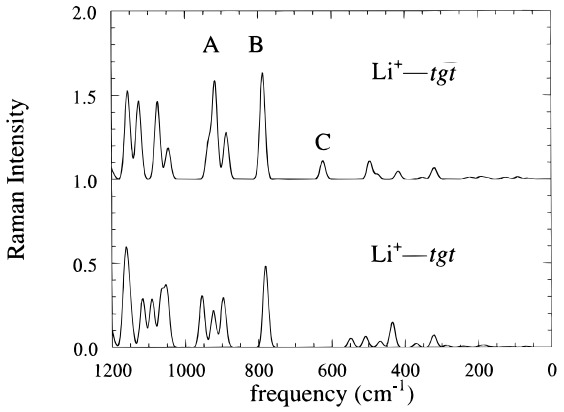

Figure 5. Calculated Raman spectra for the Li^+- $t\bar{g}t$ and Li^+-tgt complexes.

in the 770−850 cm^{-1} range. At the level of theory employed, the calculated frequencies can be expected to differ from experimental values by up to several percent. Because of this, and the similarity in frequencies of many of the conformers, and possible condensed phase shifts in frequencies, we were not able to assign the experimental Raman peaks in neat DMP liquid in the 780−850 cm^{-1} to particular conformers on the basis of the calculated frequencies and Raman activity. Examination of the neat DMP spectrum does show a very weak band at around 630 cm^{-1}. Table 5 reveals that conformers with a O-C*−C-O $\bar{g}$ conformation have a moderately strong band in this region. Therefore, we can conclude that these conformers are not important in the neat DMP liquid.

Experimentally, for the $[Li^+]/[\text{-O-}] = 0.20$ DMP/$LiCl0_4$ solution, three important bands between 500 and 1000 cm^{-1}, at about 630, 810, and 940 cm^{-1}, are observed. These bands, with their relative peak intensities (630 $cm^{-1} = 2$) are shown in Figure 4. The calculated Li^+−DMP conformer bands are also shown for the low-energy DMP conformers. Given the uncertainty in the calculated frequencies, any (or all) of the important conformers could be the source of the large peak at 810 cm^{-1}. However, the $t\bar{g}t$ and *tgt* conformers can interact much more favorably with Li^+ than any of the other important conformers, and therefore their populations would be expected to increase with increasing Li^+ concentration at the expense of the remaining conformers. We have observed such effects in simulations of DME and LiI. Additionally, only conformers with O-C*−C-O $\bar{g}$ conformations will contribute to the strong band at 630 cm^{-1} (which is weak in the neat liquid). This mode involves primarily displacements of the α carbon, the α methyl carbon, the methylene carbon, and the hydrogen atoms attached to these carbons. A mode with similar (magnitude) atomic displacements occurs in conformers with O-C*−C-O *g* and *t* conformations at around 500 cm^{-1}. This mode exhibits valence force constants similar to those seen for the higher frequency mode for the conformers with O-C*−C-O $\bar{g}$ conformations. Hence, the frequency difference can be associated with differences in geometry due to rotation about the O-C*−C-O dihedral. Because of the increase in intensity of this band with the addition of $LiClO_4$, and the fact that the quantum chemistry calculations show that Li^+- $t\bar{g}t$ complexes are at least as energetically favorable as the Li^+-tgt complexes, we conclude that Li^+- $t\bar{g}t$ complexes increase in importance in DMP/$LiClO_4$ solutions as the salt concentration increases. Whether the *tgt* population also increases with increasing salt content, as has been suggested,[14] cannot be determined conclusively from the relative complex energies and comparison of the calculated and experimental spectra.

Calculated spectra for the Li^+- $t\bar{g}t$ and Li^+-tgt complexes are shown in Figure 5. Here, each calculated mode *j* contributes

$$I_j(\omega) = \sqrt{\frac{1}{3\pi\alpha^2}} I_j \exp[-(\omega-\omega_j)^2/\alpha^2] \qquad (1)$$

to the total spectrum, where $I_j(\omega)$ is the Raman intensity due to mode *j* at frequency ω, I_j and ω_j are the calculated Raman activity and frequency of the mode, and α is a "smearing" factor. A value of $\alpha = 10$ cm^{-1}, which reproduces the full width at half maximum of the 810 cm^{-1} experimental peak for the $[Li^+]/[\text{-O-}] = 0.20$ DMP/$LiCl0_4$ solution spectrum, was used for all modes. Calculations show a moderately strong peak at 620 cm^{-1} for the $Li^+-t\bar{g}t$ spectrum, labeled "C" in Figure 5. However, the calculations do not indicate significant Raman activity in the range of the 630 cm^{-1} experimental peak in the Li^+-tgt spectrum. Hence, increase of the *tgt* population with increasing salt concentration cannot alone account for the experimental spectra.

Conclusions

Quantum chemistry studies of the energies and geometries of the important conformations of DMP and their complexes with Li^+ indicate that many of the effects controlling the conformations and complexes of DME are manifest in DMP. Attractive 1,5 $CH_3\cdots O$ electrostatic interactions are important in determining conformer energies in both molecules. As with the Li^+-tgt DME complex, the geometries of the $Li^{+-}-$ $t\bar{g}t$ and Li^+-tgt complexes of DMP allow both oxygen atoms to interact favorably with Li^+. This results in much lower energies for these complexes than are found for complexes where the ion can interact effectively with only a single oxygen atom. The latter include complexes involving conformers containing opposite sense gauche dihedral pairs. However, the presence of the α methyl group makes the conformational energy picture more complicated for DMP than DME and also strongly influences the geometries and energies of Li^+−DMP complexes. As a result of favorable interactions between the α methyl group and Li^+, the $Li^{+-}-$ $t\bar{g}t$ complex is comparable, or even lower, in energy than the Li^+-tgt conformer. While comparison of calculated and experimental Raman spectra do not allow a clear assignment of the dominant DMP conformer in DMP/$LiCl0_4$ solutions based upon the strong peak an 810 cm^{-1}, the emergence of a peak at 630 cm^{-1} with increasing salt concentration is consistent with the picture of an increasing population of the $t\bar{g}t$ conformer.

Acknowledgment. G.D.S. gratefully acknowledges support from NASA (NCC-1701) in performing this study.

References and Notes

(1) Smith, G. D.; Jaffe, R. L.; Yoon, D. Y. *J. Phys. Chem.* **1994**, *98*, 9072.
(2) Jaffe, R. L.; Smith, G. D.; Yoon, D. Y. *J. Phys. Chem.* **1993**, *97*, 12745.
(3) Smith, G. D.; Jaffe, R. L.; Yoon, D. Y. *J. Phys. Chem.*, in press.
(4) Smith, G. D.; Jaffe, R. L.; Yoon, D. Y. *J. Phys. Chem.* **1994**, *98*, 9078.
(5) Smith, G. D.; Jaffe, R. L.; Yoon, D. Y. *J. Phys. Chem.* **1993**, *97*, 12752.
(6) Smith, G. D.; Yoon, D. Y.; Jaffe, R. L. *Macromolecules* **1993**, *26*, 5213.
(7) Smith, G. D.; Jaffe, R. L.; Yoon, D. Y. *J. Am. Chem. Soc.* **1995**, *117*, 530.
(8) Smith, G. D.; Jaffe, R. L.; Yoon, D. Y. *Polym. Prepr.* **1995**, *36*, 680.
(9) Smith, G. D.; Yoon, D. Y.; Jaffe, R. L.; Colby, R. H.; Krishnamoorti, R.; Fetters, L. J. *Macromolecules* **1996**, *29*, 3462.
(10) Smith, G. D.; Jaffe, R. L., Partridge, H. *J. Phys. Chem. A* **1997**, *101*, 1705.
(11) Smith, G. D.; Borodin, O.; Pekny, M.; Jaffe, R. L.; Londono, D.; Annis, B. *Spectrochim. Acta*, in press.
(12) Sasanuma, Y. *Macromolecules* **1996**, *26*, 8629.
(13) Sasanuma, Y. *J. Phys. Chem.* **1994**, *98*, 13486.
(14) Yoon, S.; Ichikawa, K.; MacKnight, W. J.; Hsu, S. L. *Macromolecules* **1995**, *28*, 4278.
(15) *Mulliken*: A Computational Quantum Chemistry Program; Rice, J. E., Horn, H., Lengsfield, B. H., McLean, A. D., Carter, J. T., Replogle, E. S., Barnes, L. A., Maluendes, S. A., Lie, G. C., Gutowski, M., Rudge, W. E., Sauer, Stephan P. A., Lindh, R., Andersson, K., Chevalier, T. S., Widmark, P. O., Bouzida, Djamal, Pacansky, G., Singh, K., Gillan, C. J., Carnevali, P., Swope, Stephan P. A., and Liu, B., Eds.; Almaden Research Center, IBM Research Division, 650 Harry Road, San Jose, CA 95120−6099.
(16) Frisch, M. J.; Trucks, G. W.; Schlegel, H. B.; Gill, P. M. W.; Johnson, B. G.; Robb, M. A.; Cheeseman, J. R.; Keith, T.; Petersson, G. A.; Montgomery, J. A.; Raghavachari, K.; Al-Laham, M. A.; Zakrzewski, V. G.; Ortiz, J. V.; Foresman, J. B.; Cioslowski, J.; Stefanov, B. B.; Nanayakkara, A.; Challacombe, M.; Peng, C. Y.; Ayala, P. Y.; Chen, W.; Wong, M. W.; Andres, J. L.; Replogle, E. S.; Gomperts, R.; Martin, R. L.; Fox, D. J.; Binkley, J. S.; Defrees, D. J.; Baker, J.; Stewart, J. P.; Head-Gordon, M.; Gonzalez, C.; Pople, C. *Gaussian 94*, Revision B.1; Gaussian, Inc.: Pittsburgh, PA, 1995.
(17) Yoshida, H.; Tanaka, T.; Matsuura, H. *Chem. Lett.* **1996**, *8*, 637.